PRAMANA — journal of physics

Vol. 82, No. 4
April 2014
pp. 649–658

Investigation of exotic modes of spinning nuclei near ^{90}Zr

R PALIT* and S SAHA
Tata Institute of Fundamental Research, Homi Bhabha Road, Mumbai 400 005, India
*Corresponding author. E-mail: palit@tifr.res.in

DOI: 10.1007/s12043-014-0713-x; ***e*Publication:** 1 April 2014

Abstract. Recently, a digital data acquisition system with 96 channels has been set up for the Indian National Gamma Array (INGA) consisting of 24 Compton-suppressed clover detectors. The digital system provides higher throughput, better energy resolution and better stability for the multidetector Compton-suppressed clover array compared to the previous conventional system with analog shaping. A number of nuclear spectroscopic experiments have been carried out using the array. Selected results from this array will be presented which highlight different excitations of nuclei near-shell gaps.

Keywords. Closed shell nuclei; Indian National Gamma Array.

PACS Nos 23.20.En; 23.20.Lv; 27.50.+e; 29.30.Kv; 21.60.Cs

1. Introduction

Large array of high purity germanium (HPGe) detectors continues to provide new insights on the emergent properties and new symmetries of atomic nuclei with increasing angular momentum and excitation energy [1–5]. One of the fascinating topics of research in high spin gamma spectroscopy is the response of closed shell nuclei for increasing angular momentum. They provide suitable laboratory for testing the interactions of shell-model states, possible presence of high-spin isomers and help in understanding the shape transition as the high-j orbitals are occupied. The occupation of shape driving orbitals at higher spin gives rise to the emergence of regular band structure with increasing excitation energy [6]. At highest angular momentum, some of the nuclei in this region are expected to show Jacobi shape transition based on the model calculations [7]. The molecular states with large deformation owing to its cluster structure are present at high excitation energies in the neighbouring nuclei near the magic shells [8]. In particular, the excited states of nuclei near $N = 50$ closed shell have attracted a lot of attention in theoretical and experimental research. Though a number of heavy ion induced fusion reactions have been used to study nuclei near ^{90}Zr, in most of the cases the nucleus does not develop well-deformed band structure even at high excitation energy. This suggests a complex fragmentation of

the level scheme at high spin and poses experimental challenge for identifying exotic shapes at high spin [9]. To study these phenomena, a systematic study of high spin states of nuclei near ^{90}Zr have been carried out using the Indian National Gamma Array (INGA) facility. High spin states of these isotopes have been investigated using two reactions, namely, ^{28}Si+^{65}Cu and ^{13}C+^{80}Se. We have organized this paper in four sections. In §2, the experimental set-up and its new features will be highlighted. Section 3 will describe the results. Finally, the summary and future of the present work are given in §4.

2. Experimental set-up and its new features

A collaborative research facility called the Indian National Gamma Array (INGA) was initiated by Tata Institute of Fundamental Research, Inter-University Accelerator Centre, Bhabha Atomic Research Centre, Saha Institute of Nuclear Physics, Variable Energy Cyclotron Centre, UGC–DAE-Consortium for Scientific Research, and many universities in India [10]. This array (INGA) consisting of Compton-suppressed clover detectors facilitates polarization and lifetime measurements of the excited states due to the segmented structure of clovers and its higher efficiency [11,12]. The goal of the INGA is to perform high resolution discrete gamma ray spectroscopy of excited nuclei produced in different reactions for the investigation of a variety of nuclear structure phenomena, e.g., shape coexistence, magnetic/antimagnetic rotation, chiral rotations, coupling of gamma vibration with other modes, high spin states of neutron-rich nuclei in sd-shell and isomers near-shell closure [13–18]. Recently, a PCI-PXI-based digital data acquisition (DDAQ) system with 96 channels has been implemented for the Compton-suppressed clover array. Here, we present recent results on the excitation of nuclei near closed shell from the in-beam experiments using the clover array.

The detector array has the provision for 24 Compton-suppressed clover detectors arranged in a spherical geometry with six detectors at 90° and three detectors each at 23°, 40°, 65°, 115°, 140° and 157° with respect to the beam direction [19]. The picture of the array is shown in figure 1. The distance from the target to the crystal is 25 cm and

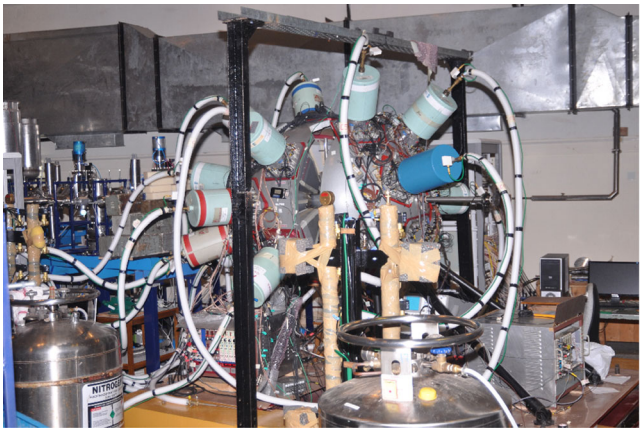

Figure 1. Picture of INGA at TIFR–BARC Pelletron Linac Facility.

the overall photopeak efficiency is around 5% at $E_\gamma \sim 1$ MeV. Each of the clover has four *n*-type crystals kept in a single cryostat.

The present digital DAQ system provides good energy resolution over the full dynamic range from 50 keV to 4 MeV of the clovers up to high count rate (∼20 kHz for each of the 96 crystals of the clover detectors). In addition, based on the time-stamping capability of the DAQ, the prompt-delayed coincidence data have been accumulated for developing new level structure above the known isomeric states. The system has the capability to provide low-fold as well as high-fold coincidence data for in-beam experiments with minimum dead time. The DDAQ has six Pixie-16 modules, two LVDS level translator modules and one controller arranged in a single Compact PCI/PXI crate. Elaborate technical information about the digitizer Pixie-16 modules can be found in [20]. Each Pixie-16 card has 16 channels and serves to 4 clover detectors. The preamplifier signal is digitized with a 12-bit 100 MHz flash analog-to-digital converter (FADC). Each of the input signal is treated in the analog circuitry for compensating the DC offset, removing the high-frequency component of the signal and amplification before passing it to the 100 MSPS digitizer. The digitized data stream of the incoming analog pulse enters the signal processing circuitry. This data stream is fed into two branches. The first branch generates a trigger through a fast filter for total multiplicity computation in the on-board field programmable gate array (FPGA). The fast trigger is generated when the fast trapezoid filter output crosses the defined threshold. The fast triggers generated from any of the 16 channels of a Pixie-16 module are distributed to its adjacent modules through the PXI backplane for generating global trigger. This fast filter, generated for forming multiplicity groups, is stretched to a pulse width of 100 ns. In the second branch, the data are passed through a delay FIFO and further branched into the energy filter for sampling the energy and trigger filter for fast trigger detection for local signal processing (e.g., pile-up detector). In the present configuration, of the six cards in a single crate, one card named as director receives and distributes the triggers among all the channels. The director computes the multiplicity and opens the coincidence window with a defined length. The veto signal of the BGO shield is given via the front panel LVDS I/O port. A valid fast trigger is generated in the absence of the veto pulse in a specific time window. In the current set-up, the first Pixie-16 module is configured to be the PXI clock master and all the modules receive the clock through the back plane.

Once the FIFO of each of the modules is ready the data are transferred to the PC in block mode and written to the respective file of the module. First, the time-stamped data from different modules are merged to a single data stream as per the 48-bit 100 MHz time-stamp and event number. The event building software 'Multi pARameter time-stamped based COincidence Search program (MARCOS)' developed at TIFR sorts the combined data stream to usual coincident events based on the mapping of DDAQ channels to different crystals of the detectors. The gains of the different crystals have been matched by the event building program by energy calibration coefficients. The event building program has the capability of making prompt gamma–prompt gamma correlations as well as the prompt gamma–delayed gamma correlation study by choosing the proper time windows as the external parameters. Conditional time spectra are also generated to look for the prompt and delayed components between different transitions.

Since the commissioning of the array at the TIFR–BARC Pelletron Linac Facility, Mumbai, a number of nuclear spectroscopic investigations have been carried out using the

array. The implementation of the coupling of the DDAQ to the INGA has been reported in [21]. Recently, a pair of degenerate dipole bands with negative parity along with the linking transitions have been established in ^{108}Ag. Comparison of the measured energy levels and ratio of the transition strengths of these bands with the calculations of the triaxial projected shell model suggest that the partner band has a different quasiparticle structure as compared to the yrast band [22]. Another highlight of the present campaign is the observation of two antimagnetic rotational bands in a single nucleus ^{107}Cd [23]. The high spin states of ^{122}I have been studied up to spin $I = 30$ and the maximally aligned states involving all eight particles outside the ^{114}Sn core have been identified [24]. Two new band structures, with six-quasiparticle configuration, have been observed in ^{194}Tl [25]. Near yrast states of ^{89}Zr were investigated up to high spin and the levels were compared with the results of the shell model calculations based on the recently developed shell model calculations [26].

3. Results on high spin states of ^{88,89}Zr nuclei

In one of the experiments, the excited states of ^{88}Zr and ^{89}Zr were populated using the ^{13}C+^{80}Se reaction. Both thin and backed target experiments were performed for the detailed spectroscopy of the high spins states. Two-fold coincidence between any of the available clovers was set for the current set-up. In the software the firing pattern of a clover was generated from the 'OR' of its four crystals and this further decides the clover multiplicity in a given event. The add-back energies of the different clovers were sorted through the 48-bit time-stamp into two-dimensional matrix and three-dimensional cube for further analysis. The gated spectra were obtained by symmetrization of the gamma–gamma matrix and gamma–gamma–gamma cube followed by Compton background subtraction using the procedure mentioned in [27]. Directional correlation of oriented states (DCO) and integrated polarization direction correlation (IPDCO) analysis of different transitions were carried out to determine the spin and parity of the excited states. The spin assignments of the various excited states reported in this paper were correlated with the generic assumption that, for the states populated in heavy-ion fusion evaporation reactions, an increase in excitation energy is usually correlated with increase in spin.

Both prompt $\gamma\gamma$-coincidence as well as prompt-delayed-$\gamma\gamma$ analysis were performed to construct the level scheme of ^{88,89}Zr. The gate width of the prompt timing was set to 200 ns. In prompt-delayed coincidence analysis, the prompt gate was set to 150 ns, while the delayed gate width was taken as 500 ns with the gate starting at 1500 ns away from the prompt. In figure 2a, the delayed spectrum generated with gate on the 1022 keV transition is shown. ^{88}Zr has an isomeric state at $E_X = 2888$ keV excitation energy and $J^\pi = 8^+$ with lifetime $T_{1/2} = 1.7$ μs [28]. The 1022 keV transition above the isomer, while used as a prompt gate in the prompt-delayed-$\gamma\gamma$ analysis, shows the 77, 272, 399, 671, 1057 and 1083 keV transitions emitted after the decay of the isomeric state (figure 2a). Similarly, figure 2b shows prompt gamma rays in coincidence with the 1022 keV transition decaying from the positive-parity excited states of ^{88}Zr above the isomer. This result demonstrates the capability of the present configuration of INGA to measure the excited states above a known isomeric state using isomer decay tagging. From our current analysis, the level scheme of ^{88}Zr have been extended mainly for the positive-parity states with the addition

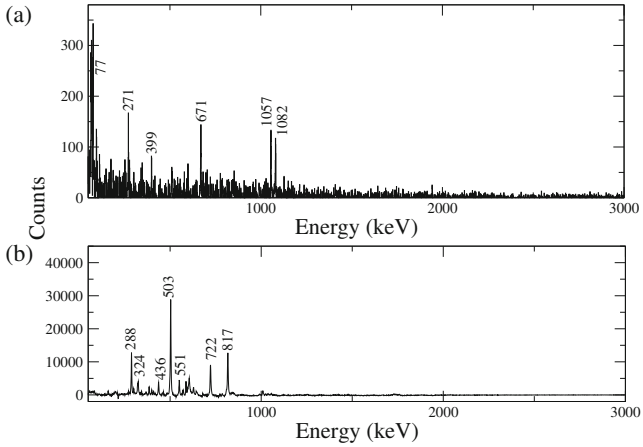

Figure 2. (**a**) Delayed spectrum gated on 1022 keV transition of ^{88}Zr and (**b**) prompt spectrum gated on 1022 keV transition of ^{88}Zr. Panel (**a**) shows the γ-rays of ^{88}Zr below the isomer, while (**b**) depicts the various transitions present above the isomer.

of many new transitions. Both the positive as well as the negative-parity states, up to the highest observed spin and excitation energy indicate the dominance of single-particle excitations in ^{88}Zr.

The knowledge of high-spin states in ^{89}Zr was very limited. The high-spin states of ^{89}Zr have been studied using the ^{88}Sr(α, $3n$)^{89}Zr, ^{76}Ge(^{16}O, $3n$)^{89}Zr and ^{74}Ge(^{18}O, $3n$)^{89}Zr reactions with smaller arrays with up to 3 HPGe detectors [29,30]. Levels of ^{89}Zr have also been studied using (p, t), (p, d), (d, t), $(p, n\gamma)$ and (^{3}He, α) reactions [31–34] apart from radioactive decay investigations [35].

A typical double gated spectrum from the present measurement is shown in figure 3. From the coincidence analysis, the excited levels of ^{89}Zr have been observed up to $\sim$12 MeV excitation energy and spin $\sim 49/2\ \hbar$. The present level scheme consists of two parts: (i) the positive-parity states up to 9602 keV excitation energy and (ii) the negative-parity states up to 12259 keV excitation energy. The 271–1744 keV double gated spectrum given in figure 3 shows the transitions including several new transitions, feeding the $13/2^+$ state of ^{89}Zr. A number of new transitions with 456, 508, 589, 600, 644, 675, 1014, 1291 and 1335 keV energies decaying from the excited states are indicated in this spectrum. The observation of several cross-over and decay-out transitions from different levels as observed in the double gated spectra helped in developing both positive- and negative-parity states. One of the interesting aspects of the present level scheme is the observation of a cascade of 10 γ-rays feeding the 6244 keV level. The DCO and polarization measurements confirm $\Delta I = 1$ and magnetic nature of the γ-rays of the cascade.

The strongly populated positive-parity states up to medium spin $(27/2^+)$ have very similar level structure to that in its nearest isotone ^{91}Mo and suggest the contribution of seniority 1 configurations as noted in [36]. To interpret the experimental data for low-lying spectra and several high spin states of ^{89}Zr, the state-of-the-art shell-model calculation using two different interactions have been performed. The calculations have been carried out in the 28–50 valence shell composed of the $1p_{3/2}$, $0f_{5/2}$, $1p_{1/2}$ and $0g_{9/2}$ orbits and

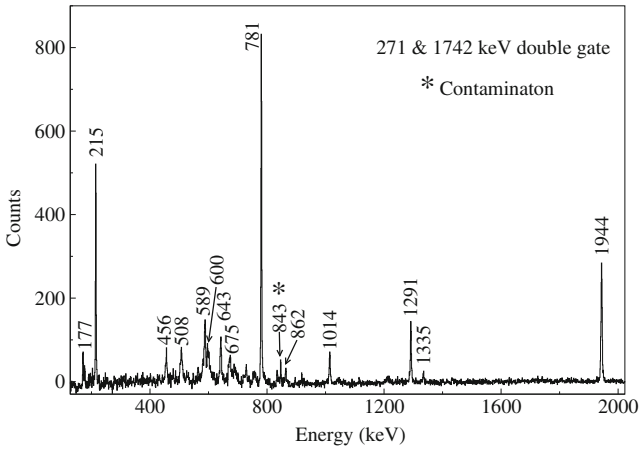

Figure 3. Spectrum obtained with double gates on 271 and 1742 keV transitions of ^{89}Zr.

employed two recently derived effective shell-model interactions, JUN45 and jj44b. The JUN45 interaction was recently developed by Honma *et al* [37]. The single-particle energies employed in conjunction with the JUN45 interaction are –9.8280, –8.7087, –7.8388 and –6.2617 MeV for the $p_{3/2}$, $f_{5/2}$, $p_{1/2}$ and $g_{9/2}$ orbits, respectively. In the case of the jj44b interaction [38], the single-particle energies are –9.6566, –9.2859, –8.2695 and –5.8944 MeV for the $p_{3/2}$, $f_{5/2}$, $p_{1/2}$ and $g_{9/2}$ orbits, respectively. The calculations were performed using the shell-model code ANTOINE [39,40]. Figure 4 shows a comparison of the experimental excitation energies of the positive-parity states of ^{89}Zr with the predictions of shell-model calculations obtained from the two sets of effective interactions. It is evident that the calculations have remarkably good agreement with the experimental results.

The ground state $9/2^+$ is well predicted by both interactions. The first excited $13/2^+$ state is well reproduced with an energy difference of 145 and 406 keV from JUN45 and jj44b interactions, respectively. The other calculated excitation energies for the levels with spin $I = 15/2^+, 17/2^+, 21/2^+, 19/2^+$ and $23/2^+$ have reasonable agreement with the experimental results. The only point of disagreement is $19/2^+$ state which is observed at the excitation energy of 3112 keV and is well predicted by JUN45 interaction but in the case of jj44b interaction it lies below $21/2^+$. The low-lying yrast states up to $25/2^+$ are well reproduced with $\pi(f_{5/2}^{(6)}p_{3/2}^{(4)}(p_{1/2}g_{9/2})^{(2)}) \otimes \nu((p_{1/2}g_{9/2})^{(11)})$ configurations contributing maximally. The non-yrast $25/2^+$ and the three $27/2^+$ states observed in the experiment have dominant contribution from seniority 3 states involving proton excitations from $p_{3/2}$ and $f_{5/2}$ orbitals to $p_{1/2}$. The decay of these states is associated with emission of high-energy transitions with energy around 2 MeV. The experimentally observed states with 6964, 7420, 8108, 8865 and 9602 keV energy up to extending spin $37/2^+$ are well described by configurations involving proton excitations from $p_{3/2}$ and $f_{5/2}$ orbitals to $g_{9/2}$. For high spin states above $25/2^+$ to $37/2^+$, the experimental results have much better agreement from JUN45 as well as jj44b interactions.

The lowest state (among the negative-parity states) observed in the present experiment is $13/2^-$ with 2121 keV energy. For this $13/2^-$ state, the difference between experiment

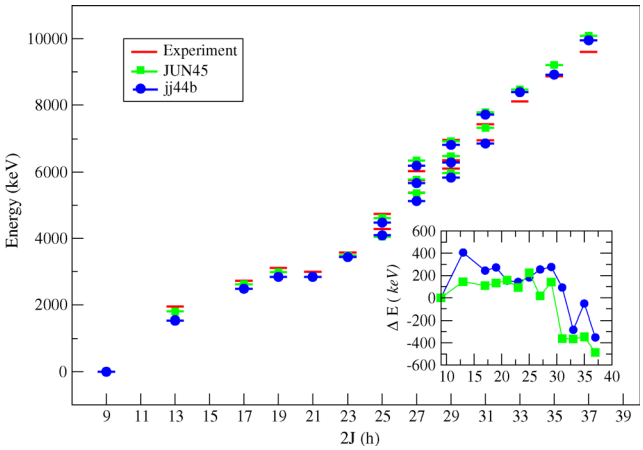

Figure 4. Experimental level scheme consisting of the positive-parity states of ^{89}Zr are compared with the large-scale shell-model calculations based on two interactions, namely, JUN45 and jj44b. The inset shows the variation of the energy difference ($\Delta E = E_{\text{expt}} - E_{\text{theory}}$) with spin for the two interactions used in the shell-model calculation.

and theory is 174 and 93 keV for JUN45 and jj44b interactions, respectively. The state has a dominant contribution from $\pi(f_{5/2}^{(6)} p_{3/2}^{(4)} p_{1/2}^{(1)} g_{9/2}^{(1)}) \otimes \nu((p_{1/2} g_{9/2})^{(11)})$ configuration. The same configuration continues to dominate up to $19/2^-$. From $21/2^-$ onwards up to $35/2^-$, the states have dominant contributions from proton excitation from $f_{5/2}$ orbital to $g_{9/2}$ which is quite well explained by the shell-model calculations.

Another interesting feature of the present work is the observation of a regular band with negative parity built on 6244 keV state with $J^\pi = 29/2^-$. The excitation energies of the excited states in the newly observed negative-parity band have been plotted with the spin values of the states indicating the emergence of rotational structure at ~6 MeV excitation energy and spin $J = 29/2$ (figure 5). This band is extended up to spin $J^\pi = 49/2^-$. In the Au-backed target data, lineshapes have been observed for many transitions in the angle-dependent matrices suggesting sub-picosecond lifetimes for many of the states. The lineshapes for the 675 keV transition as observed in the forward 65°, 90° and backward 65° angles are shown in figure 6. Comparison of the calculated lineshapes with the measured ones using LINESHAPE program [41] gives a lifetime of 0.147(14) ps for the $J^\pi = 33/2^-$ state decaying by 675 keV transition. The calculated $B(M1)$ value for the 675 keV transition is 1.26(12) μ_N^2. Similarly, the lifetime measurements for the other transitions in this band suggest their fast $M1$ nature. Further investigation about the nature of this band is under progress.

4. Summary

The performance of a fast digital data acquisition system coupled with the INGA for investigating exotic modes of spinning nuclei have been discussed. Several experiments were performed using the current set-up to investigate different high spin phenomena.

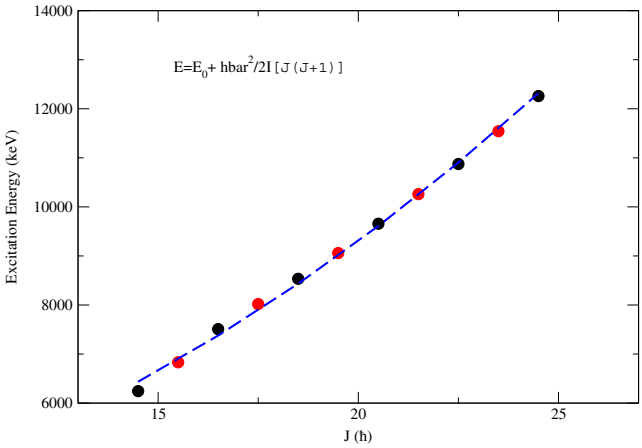

Figure 5. The excitation energies of the states in the newly observed negative-parity band have been plotted with the spin values of the states indicating the emergence of rotational structure at ∼6 MeV excitation energy and spin $J^{\pi} = 29/2^{-}$.

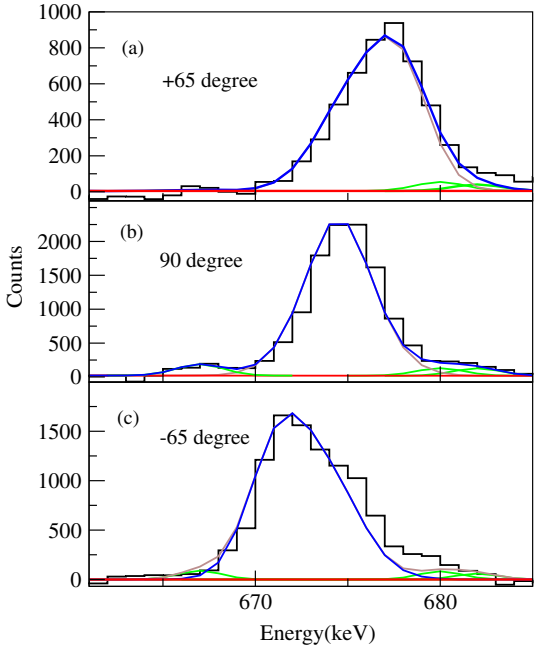

Figure 6. Experimental and theoretical lineshapes for the 675 keV transition of the negative-parity band in ^{89}Zr.

Some of the results obtained from different experiments in the current INGA campaign have also been published recently. In particular, the experimental results from the systematic study of the high spin states in ^{88,89}Zr carried out with the INGA facility are

presented. The level structures of ^{88,89}Zr are dominated with single-particle type excitation up to high spin. Interestingly, a regular band consisting of $\Delta I = 1$ magnetic transition has been observed at an excitation energy of 6244 keV. Further work in understanding the nature of the band is in progress. In future, we plan to study the high-spin states in ^{90}Zr and nearby nuclei using more symmetric reactions to study the emergence of collectivity and search for isomers at high spin.

Acknowledgements

The authors would like to thank the members of INGA Principal Investigating Coordination Committee and the INGA Collaboration for making the detectors available. The authors would also like to thank P C Srivastava for the shell-model calculation. Authors also acknowledge the IUAC group for providing some of the HV units for the clover detectors. This work was partially funded by the Department of Science and Technology, Government of India (No. IR/S2/PF-03/2003-I). The authors are thankful to the Pelletron and LINAC staff for providing excellent beam during all experiments of the campaign.

References

[1] I Y Lee, *Nucl. Phys. A* **520**, 641c (1990)
[2] J Simpson *et al*, *Heavy Ion Phys*. **11**, 159 (2000)
[3] S Frauendorf, *Rev. Mod. Phys*. **73**, 463 (2001)
J Meng and S Q Zhang, *J. Phys. G: Nucl. Phys.* **37**, 064025 (2010)
[4] B Cederwall *et al*, *Nature* **469**, 68 (2011)
[5] E A McCutchan *et al*, *Phys. Rev. Lett*. **103**, 192501 (2009)
[6] E Ideguchi *et al*, *Phys. Rev. Lett*. **87**, 222501 (2001)
[7] M Ciemala *et al*, *Acta Phys. Polonica B* **42**, 633 (2011)
[8] D C Zheng *et al*, *Phys. Rev. C* **42**, 1004 (1990)
[9] M Bunce *et al*, *Phys. Rev. C* **87**, 044337 (2013)
[10] R K Bhowmik, *Proceedings of Fourth International Conference on Fission and Properties of Neutron-Rich Nuclei* (World Scientific, 2007) 258
H C Jain, *Pramana – J. Phys.* **57**(**1**), 21 (2001)
S Muralithar *et al*, *Nucl. Instrum. Methods A* **622**, 281 (2010)
[11] R Palit, H C Jain, P K Joshi, S Nagaraj, B V T Rao, S N Chintalapudi and S S Ghugre, *Pramana – J. Phys.* **54**, 347 (2000)
[12] T Trivedi *et al*, *Nucl. Phys. A* **834**, 72c (2010)
[13] R Palit, H C Jain, P K Joshi, J A Sheikh and Y Sun, *Phys. Rev. C* **63**, 024313 (2001)
[14] S Lakshmi, H C Jain, P K Joshi, I Mazumdar, R Palit, A K Jain and S S Malik, *Nucl. Phys. A* **761**, 12 (2005)
[15] D Choudhury *et al*, *Phys. Rev. C* **82**, 061308 (2010)
[16] S Sihotra *et al*, *Phys. Rev. C* **78**, 034313 (2008)
[17] R Chakrabarti *et al*, *Phys. Rev. C* **80**, 034326 (2009)
[18] A Chakraborty *et al*, *Phys. Rev. C* **72**, 054309 (2005)
[19] R Palit, *AIP Conf. Proc.* **1336**, 573 (2011)
[20] H Tan *et al*, *Nuclear Science Symposium Conference Record*, NSS 08, IEEE, p. 3196 (2008)
[21] R Palit *et al*, *Nucl. Instrum. Methods Phys. Res., Sect. A* **680**, 90 (2012)

[22] J Sethi *et al*, *Phys. Lett. B* **725**, 85 (2013)
[23] D Choudhury *et al*, *Phys. Rev. C* **87**, 034304 (2013)
[24] P Singh *et al*, *Phys. Rev. C* **85**, 054311 (2012)
[25] H Pai *et al*, *Phys. Rev. C* **85**, 064313 (2012)
[26] S Saha *et al*, *Phys. Rev. C* **86**, 034315 (2012)
[27] D C Radford, *Nucl. Instrum. Methods A* **361**, 306 (1995)
[28] E K Warburton, J W Olness, C J Lister and R W Zurmuhle, *Phys. Rev. C* **31**, 1184 (1985)
[29] A Nilsson and M Grecescu, *Nucl. Phys. A* **212**, 448 (1973)
[30] E K Warburton, J W Olness, C J Lister, J A Becker and S D Bloom, *J. Phys. G* **12**, 1017 (1986)
[31] P Guazzoni *et al*, *Nucl. Phys. A* **697**, 611 (2002)
[32] H J Kim and R L Robinson, *Phys. Rev.* **162**, 1036 (1967)
[33] M S Greenwood, M Pluta, N Anantaraman and L R Greenwood, *Phys. Rev. C* **11**, 1995 (1975)
[34] G Duhamel-Chretien, G Perrin, C Perrin, V Comparat, E Gerlic, S Gales and C P Massolo, *Phys. Rev. C* **43**, 1116 (1991)
[35] E L Robinson, R C Hagenauer and E Eichler, *Nucl. Phys. A* **123**, 471 (1969)
[36] S Ray, N S Pattabiraman, R Goswami, S S Ghugre, A K Sinha and U Garg, *Phys. Rev. C* **69**, 054314 (2004)
[37] M Honma, T Otsuka, T Mizusaki and M Hjorth-Jensen, *Phys. Rev. C* **80**, 064323 (2009)
[38] B A Brown and A F Lisetskiy, unpublished; see also endnote (28) in B Cheal *et al*, *Phys. Rev. Lett.* **104**, 252502 (2010)
[39] E Caurier, G Martínez-Pinedo, F Nowacki, A Poves and A P Zuker, *Rev. Mod. Phys.* **77**, 427 (2005)
[40] P C Srivastava and M J Ermamatov, *Phys. Atomic Nuclei* **76**, 692 (2013)
[41] J C Wells, ORNL Physics Division Progress, Reprt No. ORNL-6689, September 30 (1991)